High-resolution Doppler-free two-photon spectroscopic studies of molecules. II. The ν_2 bands of $^{14}NH_3$†

William K. Bischel* and Patrick J. Kelly‡
Department of Applied Science, University of California, Davis–Livermore, California 94550

Charles K. Rhodes*
Lawrence Livermore Laboratory, University of California, Livermore, California 94550
(Received 24 November 1975)

Detailed studies involving high-resolution Doppler-free two-photon spectroscopic measurements of the ν_2 vibrational bands in $^{14}NH_3$ are presented. Using the technique of combining fixed-frequency ir sources with molecular Stark tuning presented in the preceding paper, we have used two successive $Q(5,4)$ vibrational-rotational transitions to study the spectroscopic and collisional properties of the ν_2 vibrational manifold. We report (1) precise transition energies for the $(\nu_2,J,K) = (0^-,5,4) \rightarrow (2^-,5,4)$ two-photon transition, (2) pressure-broadening and pressure-shift data, (3) optical Stark shift parameters, and (4) excited-state transition matrix elements. An observation of collisional narrowing arising from $^{14}NH_3$-Ne collisions is also reported.

I. INTRODUCTION

It has been demonstrated[1] that Doppler-free two-photon absorption (DFTPA) can be an extremely useful tool for investigating the spectroscopic and collisional properties of molecular systems. In this paper, we extend the techniques presented in Ref. 1 to the study of the ν_2 vibrational bands in $^{14}NH_3$. These studies not only provide detailed information about the spectroscopic and collisional properties of this molecular system, but they are also of interest for more applied reasons. There is great interest in the absorption spectrum of the ν_2 bands in NH_3, since they determine the opacity of the Jovian atmosphere at wavelengths from 8.5 to 12.5 μm.[2,3] These data are also relevant to methods of optical down conversion.

NH_3 has a number of factors in its favor for the observation of Doppler-free two-photon absorption. Among the most important are (1) the availability of reasonably extensive spectroscopic data on the 10-μm bands,[4-6] (2) large transition dipole moments,[7] and (3) a low rotational partition function. The latter two factors are important in enhancing the two-photon amplitude leading to absorption cross sections which are many times larger than those reported for CH_3F.[1] This enhancement allows a determination of several transition dipole moments not observable for lower signal-to-noise ratios. Since the theoretical considerations of DFTPA were presented in the preceding paper,[1] we will start here with an explanation of the two-photon transition in $^{14}NH_3$.

II. EXPERIMENT

A. $^{14}NH_3$ two-photon transition

NH_3 is a pyramidal molecule with the N atom approximately 0.38 Å above the plane of the three hydrgens and the N-H distance approximately 1.02 Å in the ground state.[8] Because of its threefold axis of symmetry, it also belongs to point group C_{3v}. It has four vibrational fundamentals, two symmetric (ν_1 and ν_2) and two doubly degenerate (ν_3 and ν_4). A partial vibrational energy-level diagram for the various fundamental and combination bands[4-12] is shown in Fig. 1. As indicated in this figure, each vibrational level is split into a symmetric (s or +) and an antisymmetric (a or −) state. The inversion frequency increases with vibrational quantum number v and is largest for the ν_2 mode. It should be noted that the $2\nu_2$ and ν_4 levels are nearly in resonance and coupled by Coriolis effects. This Coriolis interaction is known to induce strong perturbations between the two vibrations,[13] causing substantial mixing of these two states for particular rotational levels.

The vibrational ν_2 mode of NH_3 is a parallel band which involves the symmetric deformation of the N-H bonds. This band has a strong Q branch at ~10.6 μm favoring the nearly resonant coupling of CO_2 radiation, which enables the observation of DFTPA. From a detailed search for the available spectroscopic data of the fundamental and first-overtone bands of this mode, we were able to find close coincidences of the $P34$ and $P18$ 10.6-μm laser lines with two consecutive Q transitions with

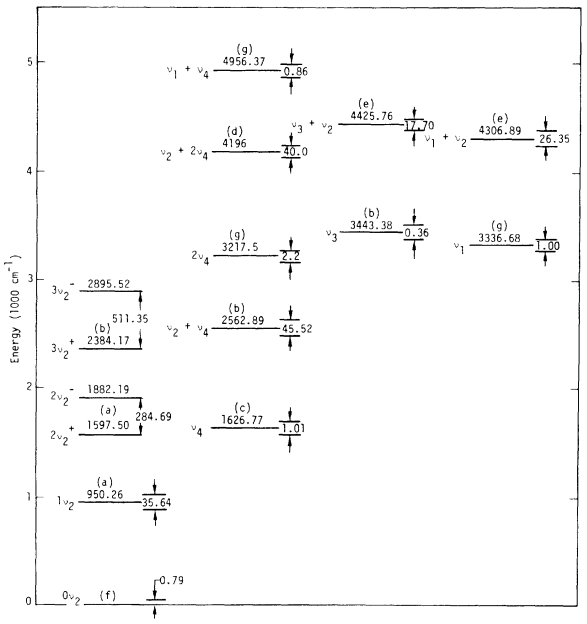

FIG. 1. Partial energy-level diagram of NH_3 illustrating several fundamental and combination vibrational states. The inversion splitting is indicated for each level. Detailed information on each level can be found in (a) Refs. 2, 4, and 6, (b) Ref. 7, (c) Ref. 4, (d) Ref. 9, (e) Ref. 10, (f) Ref. 11, and (g) Ref. 12.

$J=5$, $K=4$. This search was facilitated by the excellent Stark spectroscopy of Shimizu[5] on the $0^- \rightarrow 1^+$ vibrational band. The second transition, $1^+ \rightarrow 2^-$, was much less accurately known (±1 GHz).[4] Since the inversion splitting is very small for the ground state, almost all of the Stark tuning originated from these levels. From Sec. II C, we see that the 0^- vibrational level increases in energy only with increasing Stark field. This means that if the sum of the two CO_2 photons is *above* the upper 2^- vibrational level, the two-photon transition would never be tuned into resonance. However, the opposite situation prevailed and a two-photon transition in NH_3 was found. A detailed diagram of the levels involved in the transition is given in Fig. 2. It was found from these measurements that this transition was 294 MHz off-resonance and could be Stark tuned into resonance with a field of 5253 V/cm.

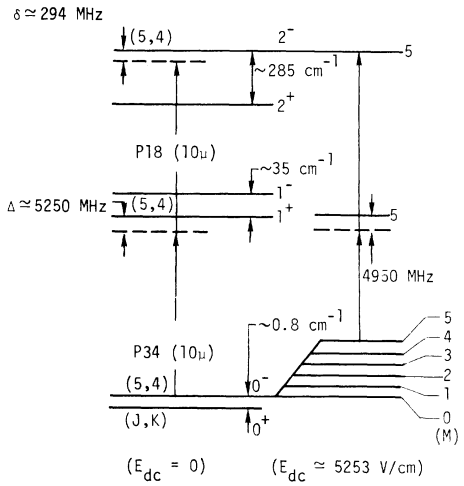

FIG. 2. Two-photon transition in the ν_2 bands of $^{14}NH_3$ for the case of $\Delta M=0$. This transition can be tuned into resonance with a Stark field of 5253 V/cm. The $P18$ (10 μm) and $P34$ (10 μm) CO_2 transitions are assumed to be at their respective center frequencies.

B. Estimate of two-photon absorption cross section in NH_3

In order to estimate the two-photon absorption cross section for NH_3, we used Eq. (21) of Ref. 1,

$$\sigma(\nu_2)=[(2\pi)^3/\hbar c^2]\, I_1 \nu_2 |P_{fg}|^2 g(\nu_1+\nu_2), \qquad (1)$$

where I_1 is the intensity of the pump radiation field, $g(\nu_1+\nu_2)$ is the normalized line-shape function for the transition, and

$$P_{fg}=\langle f|\hat{E}\cdot\vec{\mu}\,|i\rangle\langle i|\hat{E}\cdot\vec{\mu}\,|g\rangle/(E_n-h\nu_1)$$

for one dominant intermediate state. Using the appropriate parameters listed in Table I, we see that

$$\sigma/I_1 = 3.78\times10^{-20}\ \text{cm}^2/(\text{W cm}^{-2}).$$

TABLE I. Two-photon absorption intensity estimates in $^{14}NH_3$.

Molecule (transition) $(J_gK_gM_g) \rightarrow (J_iK_gM_i) \rightarrow (J_fK_gM_f)$	$\lvert\mu_{gi}\rvert^2$ (D^2)	$\lvert\mu_{if}\rvert^2$ (D^2)	ΔE (MHz)	$g(\nu_1+\nu_2)$ $=0.94/\Delta\nu_D$ (10^{-6} sec) [a]	σ/I_1 [$\text{cm}^2/(\text{W cm}^{-2})$]	N_g-N_f (cm^{-3}) at 10 mTorr	I_1 (W/cm^2)	L (cm)	$\Delta I_2/I_2=\alpha L$
NH_3 (5, 4, 5) $\rightarrow$ (5, 4, 5) $\rightarrow$ (5, 4, 5)	0.026	0.030	4950	0.701	3.78×10^{-20}	4.80×10^{11}	375	17.5	1.2×10^{-4}

[a] Residual Doppler width $\Delta\nu_D$ is calculated from Eq. (32) of Ref. 1.

This gives an absorption $\Delta I_2/I_2 \simeq 1.2\times10^{-4}$ for 10 mTorr of NH_3 pressure in our experimental configuration. Comparing this to the values for CH_3F given in Ref. 1, it is interesting to note that for the same pressure the two-photon absorption coefficient is 40 times larger for the case of NH_3; this fact was verified experimentally by the relative signal intensities. This results essentially from three factors: (1) The energy difference between the first CO_2 photon and the intermediate state is smaller, resulting in a greater resonant enhancement for NH_3, (2) the relevant transition dipole matrix elements are larger in NH_3 than in CH_3F, and (3) the population of a given rotational-vibrational level in NH_3 is larger than in CH_3F. This results from the greater rotational spacing in NH_3 leading to a smaller rotational partition function.

It is interesting to note that polarization effects between the radiation and Stark fields ($\Delta M = 0, \pm1$) play an important role in the direction-cosine matrix elements in P_{fg}. For example, the case of two photons polarized perpendicular to the Stark field will lead to an absorption cross section which is reduced by a factor of 100 below the value given in Table I.

C. Stark shift in NH_3

In discussing the Stark effect in NH_3, we must take into account the fact that each vibrational level of the ν_2 mode is split by inversion, as shown in Fig. 2. Therefore we must treat this as a special case of two "interacting" levels whose energy separation is much less than between either one and any third level. For two such close levels, the energy owing to the field cannot be considered a small perturbation; thus an exact solution is necessary. The result of this calculation[11] is expressed as

$$\Delta W^{(1)}(\mathrm{MHz}) = \pm\tfrac{1}{2}\left[(\nu_{\mathrm{inv}}^2 + x^2)^{1/2} - \nu_{\mathrm{inv}}\right] \tag{2}$$

where

$$x = 2\mu EMK\, a/J(J+1) \tag{3}$$

and $a = 0.503\,48$ such that $\mu \cdot E(\mathrm{MHz}) = 0.503\,48\,\mu(\mathrm{D}) \times E(\mathrm{V/cm})$. Here, ν_{inv} is the inversion frequency and the $\pm$ sign corresponds to the upper or lower of the inversion levels, respectively. Equation (2) is an exact expression for the Stark effect arising from the two inversion states. The interaction of the nearby rotational states ($J' = J \pm 1$) produces additional shifts that can be calculated from second-order perturbation theory. These are given by[5,14]

$$\Delta W^{(2)}(\mathrm{MHz}) = a^2\mu^2E^2\left(\frac{(J^2-K^2)(J^2-M^2)}{(2BJ\pm\nu_{\mathrm{inv}})J^2(2J-1)(2J+1)} + \frac{[(J+1)^2-K^2][(J+1)^2-M^2]}{[-2B(J+1)\pm\nu_{\mathrm{inv}}](J+1)^2(2J+1)(2J+3)}\right). \tag{4}$$

For the lower state ($\nu_2 = 0$), the Stark shift must be calculated by combining Eqs. (2) and (3). However, for the upper vibrational level ($\nu_2 = 2$) one may use an approximation for Eq. (2), since $x \ll \nu_{\mathrm{inv}}$. In this case, the first-order term becomes

$$\Delta W_f^{(1)}(\mathrm{MHz}) \simeq \tfrac{1}{4}x^2/\nu_{\mathrm{inv}}. \tag{5}$$

Since this term is generally small, we will combine it with the second-order terms for the upper state given by Eq. (4). Since the overall tuning of the two-photon transition is the difference between the tuning of the individual levels, we can write the total Stark shift as

$$\delta W' = \Delta W_g^{(1)} + \Delta W_g^{(2)} - \Delta W_f^{(2)}. \tag{6}$$

Substituting Eq. (2) for $\Delta W_g^{(1)}$, Eq. (4) for $\Delta W_g^{(2)}$, and Eqs. (4) and (5) for $\Delta W_f^{(2)}$, we have

$$\delta W'(\mathrm{MHz}) = \tfrac{1}{2}\left[(\nu_{\mathrm{inv}}^2 + x^2)^{1/2} - \nu_{\mathrm{inv}}\right]_g + D_3\mu_g^2E^2 - D_4\mu_f^2E^2, \tag{7}$$

where D_3 is defined by Eq. (4) using the plus sign and D_4 is defined by a sum of Eqs. (4) and (5) using the plus sign. Values for D_3 and D_4 for the three $\Delta M = 0$ Stark transitions observed in NH_3 are given in Table II. It is interesting to note from Eq. (2) that each Stark-shifted level is now doubly degenerate owing to the $\pm M$ degeneracy. This should be compared to the nondegenerate Stark-shifted levels for the case of CH_3F [Eq. (43) of Ref. 1].

In order to accurately find the two-photon transition frequency, two correction terms must be added to Eq. (7). The first correction is experimental. In determining a particular resonance we set the dc Stark field at a constant value, offset one of the lasers (the $P34$ line) 500 kHz below its center frequency, and sweep the other laser ($P18$) line through the two-photon resonance. These frequency offsets corresponding to the center of the two-photon resonance are tabulated in Table III. The other correction involves the level shifts (power shifts) induced by the optical fields of the lasers. This term (δW_E) is calculated in Sec. IV C and tabulated in Table VI. Equation (6) may now be written

$$\delta W = \Delta W_g^{(1)} + \Delta W_g^{(2)} - \Delta W_f^{(1)} + \delta W_L + \delta W_E, \tag{8}$$

where δW is now referenced to the center of the CO_2 laser lines. Tabulated values for δW may be found in Table II. Note that our calculated values

TABLE II. Evaluation of resonant Stark shift in NH_3. [a]

Transition M_g	Transition M_f	E [b] (V/cm)	$\Delta W_g^{(1)}$ (MHz)	$D_3\mu_g^2\times10^{9}$ [c] [MHz/(V^{2}cm^{-2})]	$\Delta W_g^{(2)}$ (MHz)	$D_4\times10^{8}$ [d] [MHz/(V^{2}cm^{-2}) D^2]	$\Delta W_f^{(2)}$ [e] (MHz)	δW_L (MHz)	δW_E [f] (MHz)	δW (MHz)
5	5	5253.40	294.786	−6.627 49	−0.183	1.561 10	0.297	−0.021	0.071	294.36
4	4	6580.43	295.999	−6.043 64	−0.262	1.339 44	0.400	−0.993	0.045	294.39
3	3	8772.34	295.895	−5.589 52	−0.430	1.167 03	0.619	−0.517	0.026	294.36
									Average	394.37

[a] See Eq. (7) for definition of column symbols.
[b] Plate spacing of 0.496 48 cm.
[c] $B(\nu_2=0^+)=9.9463$ cm^{-1} (Ref. 6); $\nu_{\rm inv}(\nu_2, J, K=0, 5, 4)=0.7551$ cm^{-1} (Ref. 11); $\mu_g=1.475$ D (Table V).
[d] $B(\nu_2=2^+)=10.261$ cm^{-1}, $\nu_{\rm inv}(\nu_2, J, K=2, 5, 4)=281.66$ cm^{-1} (Ref. 4).
[e] $\mu_f=0.83$ D (see Table V).
[f] $\delta W_E=\Delta W_{Eg}-\Delta W_{Ef}$. These values are tabulated in Table VI.

for the three independently measured ($\Delta M=0$) transitions (δW) differ from the average value of $\delta W=294.37$ MHz by a maximum of only 20 kHz. This close agreement between theory and experiment is encouraging and testifies to accuracy attainable with this technique of measurement. Combining this Stark shift with the CO_2 laser gives a value for the frequency of the two-photon transition $(\nu_2, J, K)=(0^-, 5, 4)\rightarrow(2^-, 5, 4)$ of 1876.991 493 $\pm3\times10^{-6}$ cm^{-1}. This is unquestionably the most accurately determined value for a two-photon transition.

D. NH_3 data presentation and analysis

The general experimental setup was again that described in Sec. III D of Ref. 1. Throughout the NH_3 experiments, however, there were some problems not present for the case of CH_3F. Since the Stark voltage was much higher to obtain resonance, the problem of gas breakdown was present. The highest pressure attainable in the cell at these high voltages for the plate spacing of 5 mm was only 40 mTorr. This pressure was not sufficient for detailed pressure-broadening studies. This problem was partially alleviated by going to a smaller plate spacing of 2.2 mm. This new plate spacing was calibrated by taking the ratios of the new voltages determined for the three $\Delta M=0$ transitions to the old voltages times the old plate spacing which was calibrated from the CH_3F data. This determined a new value for the plate spacing of $d=0.219\,74\pm0.000\,10$ cm. With this spacing we were able to obtain pressures of 80–100 mTorr for the self-broadening case.

We also added a small amount (2–3 mTorr) of SF_6, a material with favorable dielectric properties which strongly inhibited the breakdown phenomenon. However, an alternate problem appeared, as the threshold voltage for corona was substantially reduced by the SF_6. This behavior limited the total pressure range that could be examined, but the combination of the lower plate spacing and the SF_6 allowed sufficient data to be obtained for pressure-broadening studies.

A significant practical problem arises from the fact that NH_3 is very adhesive to the interior walls of the absorption cell. This aspect interfered with determinations of accurate partial pressures of NH_3 and foreign-gas perturbers. This difficulty was eliminated by first flushing the cell with high-pressure NH_3 (several Torr) and then filling the cell to the appropriate pressure and waiting at least 30 min for the pressure to reach equilibrium. This procedure insured accurate NH_3 partial pressures.

A sample of the data obtained in NH_3 using an experimental procedure similar to the one outlined in the preceding paper is given in Fig. 3. As in the case of CH_3F, there is no Doppler background owing to separate beam two-photon absorption, since the frequencies $2\nu_1$ and $2\nu_2$ are several hundred Doppler widths off the two-photon resonance. The analytical procedure used to reduce the NH_3 data was simplified somewhat from the one used for CH_3F. As can be seen from Fig. 3, the signal-to-noise ratio is extremely high for NH_3, allowing the data to be taken using a very small modulation amplitude. Thus modulation broadening did not complicate the data reduction. This allowed the experimental linewidths to be fitted directly with the derivative of Voigt profile. This fit is indicated

TABLE III. Laser Frequency offsets corresponding to the observed two-photon resonances for Stark fields given in Table V.

Transition M_g	Transition M_f	$P18$ (kHz)	$P34$ (kHz)	δW_L (MHz)
5	5	+479	−500	−0.021
4	4	−493	−500	−0.993
3	3	−17	−500	−0.517

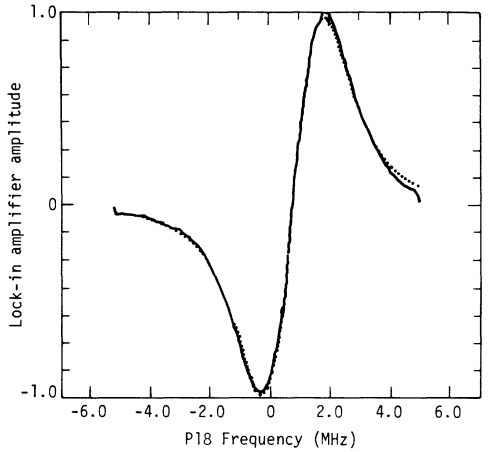

FIG. 3. Two-photon absorption signal from NH_3 using the transition in Fig. 2. The probe oscillator ($P34$) was locked 500 kHz below line center while the pump oscillator ($P18$) was swept through the line. The NH_3 pressure was 42 mTorr and the peak-to-peak modulation amplitude was 0.293 MHz. Note the slight asymmetry in the line shape which could be attributed to unresolved hyperfine splittings. Dotted line: Best fit to the derivative of the Voigt profile giving a total width of 3.14 MHz and a homogeneous contribution of 2.52 MHz.

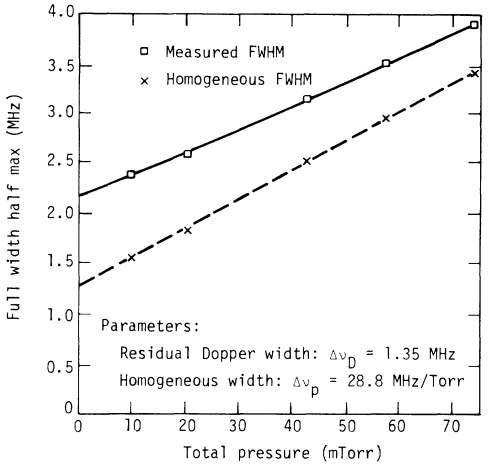

FIG. 4. NH_3 self-broadening data for the two-photon transition $(J,K,M) \rightarrow (J',K',M') = (5,4,5) \rightarrow (5,4,5)$. The two laser fields were polarized parallel to the Stark field. The data were established by a fit with the derivative of the Voigt profile.

by the dotted line in Fig. 3. The numerical procedure calculating this derivative was originally used to evaluate the plasma dispersion function.[15] From this analysis, we obtain homogeneous linewidths which were automatically stored for the various pressures and subsequently fitted to a straight line, thereby determining the pressure-broadening coefficient.

Pressure-broadening coefficients were obtained for the cases of self-broadening and broadening by the foreign-gas perturbers H_2, D_2, He, Ne, and Xe. A sample plot of the data is given in Fig. 4 for the case of self-broadening in NH_3. Note that the homogeneous contribution to the linewidth does not extrapolate to zero, as was the case for the data taken in CH_3F (Fig. 5 of Ref. 1). One explanation for this observation might be that unresolved hyperfine splittings[11,16] are contributing to the total linewidth. Also, power-broadening and power-shift[17] contributions to the linewidths are no longer negligible and could account for part of the zero-pressure value of the homogeneous linewidth.

A tabulation of all of the experimentally determined linewidths is given in Table IV. A general interpretation of these data in terms of the molecular collisional process is left to Sec. III. It is interesting to note the existence of anomalous effects in the NH_3–rare-gas–broadening data. The most pronounced effect is seen in Fig. 5 for the case of NH_3-Ne collisions. We observe in this case that the linewidth at low pressure actually narrows (line S_2), while the higher-pressure points indicate a broadening at a very low rate (line S_1). Similar effects can also be seen in the *low-pressure* NH_3-He data, where a very low broadening coefficient is observed (see Table IV). These effects can be interpreted in a manner after Dicke[18] and are discussed in Sec. III C.

One final comment concerning these data for the case of NH_3-Xe is in order. Pressures higher than 50 mTorr were unobtainable because of breakdown and corona problems. The data obtained for the lower pressures give a low broadening coefficient. The error bars on this coefficient are fairly large and the reported value should be taken as correct only within a factor of 2.

III. COLLISIONAL PROPERTIES OF $^{14}NH_3$

A. Pressure broadening in NH_3

During the last thirty years, the pressure broadening of NH_3 microwave transitions has been extensively studied both experimentally and theoretically. Anderson[19] was the first to obtain reasonably good agreement between his theoretical treatment and the data of Bleaney and Penrose.[20] A good review of this earlier work is given by Townes and Schawlow.[11] Assuming the dominant collisional processes in NH_3 are dipolar transitions between the inversion doublet, Anderson predicts a linewidth dependence on rotational state (J,K)

$$\Delta\nu_p \propto |K|/[J(J+1)]^{1/2}. \quad (9)$$

Although Bleaney and Penrose obtained the closest fit to their experimental data by using Eq. (9) to the $\frac{1}{3}$ power, we will assume the rotational-state de-

TABLE IV. Comparison of experimental pressure-broadening parameters in $^{14}NH_3$ for the two-photon transition $(\nu_2, J, K, M) \rightarrow (\nu_2', J', K', M') = (0^-, 5, 4, 5) \rightarrow (2^-, 5, 4, 5)$.

Perturber	Experimental linewidth ($\Delta\nu_p$) (FWHM) (MHz/Torr)	Experimental optical-broadening cross section[a] b_e (Å)	σ' (Å^2)	Gas kinetic cross section[b] b_e (Å)	σ' (Å^2)	Reduced mass (μ) (amu)	Relative velocity[a] (v_{rel}) ($\times 10^5$ cm/sec)
NH_3	28.8 ±1.0	10.2	325	4.43	61.7	8.50	0.864
H_2	4.74± 0.25	2.80	24.6	3.68	42.5	1.789	1.88
D_2	4.32± 0.25	3.10	30.1	3.68	52.5	3.24	1.40
He	1.44± 0.15	1.79	10.0	3.50	38.4	3.24	1.40
Ne	0.57± ?	1.46	6.70	3.61	40.9	9.189	0.830
Xe	1.8 ± ?	2.93	27.1	4.24	56.5	15.04	0.649

[a] The conversion formulas used to calculate these values can be found in Table IV of the preceding paper (Ref. 1).
[b] Kinetic diameters are those obtained from Joseph O. Hirschfelder, Charles F. Curtis, and R. Byron Bird, *Molecular Theory of Gases* (Wiley, New York, 1954). The kinetic diameters for mixtures are obtained from the usual combination rule, $b = \frac{1}{2}(b_1 + b_2)$.

pendence shown in Eq. (9), since Anderson has shown that the assumptions used by Bleaney and Penrose to derive their result were incorrect.

We begin by comparing our widths to other published data of transitions in the microwave and infrared. A tabulation of the microwave linewidths determined before 1955 can be found in Ref. 11. Other measurements used for comparison are the work of Legan *et al.*[21] and Kakar and Poyneter.[22] The values given by Legan are the result of a careful and systematic investigation with corrections included for modulation broadening, cell length, and even Doppler broadening at low pressures. Although these values are consistantly lower than those given by Bleaney and Penrose, we will assume these are the correct values. Since the broadening coefficient can vary by as much as 50%, depending on the rotational state (J,K), it is necessary to compare our transition $[Q(5,4)]$ to other determinations using the same rotational states. Unfortunately, there are little data useful for a direct comparison. However, assuming a linewidth dependence on J,K, as in Eq. (9), one can extrapolate the microwave data with reasonable accuracy to obtain a broadening coefficient of about 44.0 MHz/Torr for the $Q(5,4)$ transition. Note that our determination for the two-photon $Q(5,4)$ transition ($\Delta\nu_p = 28.8$ MHz/Torr) is much smaller.

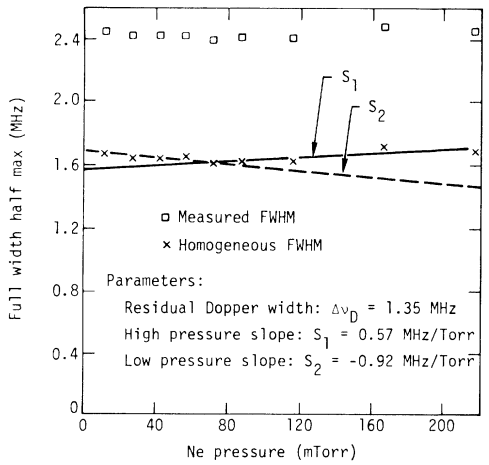

FIG. 5. First observation of collisional narrowing effects in two-photon absorption spectra. Line S_1 is the straight-line fit to the high-pressure points (> 100 mTorr) and gives an anomalously small broadening coefficient. The slope of line S_2 is actually negative, indicating collisional narrowing is occurring. The total narrowing observed is ~ 70 kHz.

Data for infrared transitions are even more sparse. A few line-broadening parameters have been measured by Varanasi,[23] Mattick *et al.*,[24] Shimizu,[7] and Benedict *et al.*[8] Comparing these determinations to available microwave data, we find that the infrared-broadening coefficients are generally 10–20% less than the corresponding microwave coefficients. From these comparisons, we can obtain a general trend: As the ν_2 vibrational quantum number increases, the linewidth narrows.

To understand this narrowing, one must first look at the basic collisional processes allowed in NH_3. Assuming the collisional interactions in the upper and lower states are statistically independent, we can approximate the linewidth as[7]

$$\Delta\nu_p = \frac{1}{2\pi}\left(\frac{1}{T_L} + \frac{1}{T_u}\right). \tag{10}$$

Normally, it is assumed that $T_L = T_u$. This assumption should be reasonably accurate for microwave broadening but could change drastically for infrared broadening, since the character of the upper state is much different from the lower state. In general, the linewidth is a combination of contributions from different types of collisional pro-

cesses which perturb the phase but do not change the state, reorient the angular momentum vector, or change the rotational state. The general selection rules for dipole-dipole type transitions (expected for CH_3F and NH_3 self-broadening) are

$$+ \rightleftarrows -, \quad \Delta J = 0, \pm 1, \quad \text{and} \quad \Delta M = 0, \pm 1.$$

These selection rules have been verified for NH_3 by Oka.[25] If we assume a linewidth model as in Eq. (10), the variances in the linewidth could be explained by a reduced collision frequency in the upper state. To illustrate this point, we compare the collisional processes for CH_3F and NH_3.

In the case of CH_3F, the vibrational states are doubly degenerate (±). Hence collisional processes which require little or no energy change (types a and b) can occur and contribute to a substantial portion of the linewidth. This has been verified by Johns *et al.*,[26] who estimate that reorientation collisions ($\Delta M = \pm 1$) can account for up to 70% of the linewidth. Also, since the B constants are almost the same for upper and lower states, the contribution from rotationally inelastic collisions should be the same. This means that we would expect linewidth comparable to the microwave data, an expectation which is supported by the data.

NH_3, however, is a completely different case. Here the vibrational levels have an inversion splitting which rapidly increases with ν_2 quantum number. Since the dipole selection rule is $+ \rightleftarrows -$, the only allowed dipole-type collisions must occur between the inversion doublets. For the ground state, the splitting is only 0.8 cm^{-1}. Hence energy can easily be exchanged between these states and nearly resonant dipolar transitions can occur. However, for the $\nu_2 = 1$ level, the splitting is 35 cm^{-1}, leading to a much larger energy deficit to be converted into translational energy. Thus these partially resonant collisions have a smaller broadening cross section, giving $T_L < T_u$ and a smaller linewidth.[27] For the $\nu_2 = 2$ mode, the inversion splitting is 280 cm^{-1}, a value which is somewhat larger than the average thermal energy ($kT \cong 200$ cm^{-1}). Also, for $J = 5$, the rotational line spacing is $2BJ \cong 100$ cm^{-1}, which means that a rotational transition $J \rightarrow J+1$ is still ~180 cm^{-1} off-resonance. Hence any dipole collisional process would be completely nonresonant and would have a very small transition probability. To zeroth order we could assume the upper state contribution to be zero and hence expect a 50% reduction in width. Qualitatively, dramatic reductions in the widths are observed, which in this model can be attributed directly to the dipole-dipole selection rules. Note that in the dipole approximation there is no contribution from reorientational collisions. We can expect some residual contribution to the linewidth from inversion state changes in the $\nu_2 = 2$ state, but the major effect is probably due to reorientation collisions from the quadrupole-dipole interaction term in the intermolecular potential, since the vibrational selection rules for these types of collisions are $+ \rightleftarrows +$ and $- \rightleftarrows -$. However, NH_3 has a relatively small quadruple moment (1.30 D Å) and a detailed calculation would have to be performed to extract the relative contribution. Johns *et al.*[26] have demonstrated that reorientational collisions do occur in NH_3 and make up approximately 7% of the linewidth. Benedict *et al.*[8,10] propose a similar explanation for decreases in the widths of lines in combination band spectra.

Foreign-gas broadening in NH_3 has been as extensively studied as self-broadening. One reason for the interest in NH_3 is that Smith[28] concludes that the NH_3 inversion spectrum is more useful than the rotational spectra of linear molecules for the purpose of evaluating the quadrupole moments of foreign-gas perturbers. This conclusion is predicated on the fact that competing interactions involving the polarizability of the collision partner are much smaller for ammonia than for linear molecules. A large number of quadrupole moments have been determined from NH_3 line-broadening data.[29]

It is interesting to note the velocity dependence of the linewidths for dipole-quadrupole forces. Following the treatment in Townes and Schawlow,[11] we see that the line-broadening parameter ($\Delta\nu_p$) can be related to the relative velocity (v_{rel}), using Anderson's theory, by

$$2\pi\Delta\nu_p = N v_{\text{rel}}\,\sigma \propto N v_{\text{rel}}^{1/2(n-1)}, \tag{11}$$

where n is related to the specific term in the multipole expansion of the intermolecular potential and σ is the velocity-dependent collision cross section. For dipole-quadrupole forces $n = 4$, hence

$$\Delta\nu_p \propto v_{\text{rel}}^{1/3}.$$

Note that there is no velocity dependence of the linewidth for dipole-dipole forces ($n = 3$). This has been beautifully demonstrated by Mattick *et al.*[24] for the case of self-broadening in NH_3.

We now compare the velocity dependence of the linewidth for the case of broadening of NH_3 by H_2 and D_2, assuming a dipole-quadrupole interaction force. Since both of the molecules have the same quadrupole moment,[29] we would expect from the previous discussion that the radio of the linewidths would go as

$$\frac{\Delta\nu_{H_2}}{\Delta\nu_{D_2}} = \left(\frac{v_{H_2}}{v_{D_2}}\right)^{1/3} = \left(\frac{\mu_{D_2}}{\mu_{H_2}}\right)^{1/6},$$

since the relative velocity is related to the reduced mass by $v_{\text{rel}} \propto 1/\mu^{1/2}$. With $\mu_{D_2} = 3.24$ and $\mu_{H_2} = 1.79$

amu,

$$\Delta\nu_{H_2}/\Delta\nu_{D_2} = (3.24/1.79)^{1/6} = 1.10.$$

Taking the appropriate measured linewidths from Table IV, we see that

$$\Delta\nu_{H_2}/\Delta\nu_{D_2} = 4.74/4.32 = 1.10,$$

which provides very strong support to the assumption that the main interaction in NH_3-H_2 collisions is the dipole-quadrupole term. Anderson[27] suggested that the main part of the linewidth for NH_3-H_2 collisions could be accounted for by the quadrupole-induced dipole term ($n=7$) in the intermolecular potential. The polarizabilities of H_2 and D_2 are the same, so we again can compare the velocity dependence of this term. Using Eq. (11) we have

$$\Delta\nu \propto v_{rel}^{2/3},$$

giving

$$\frac{\Delta\nu_{H_2}}{\Delta\nu_{D_2}} = \left(\frac{v_{H_2}}{v_{D_2}}\right)^{2/3} = \left(\frac{\mu_{D_2}}{\mu_{H_2}}\right)^{1/3} = 1.21.$$

Since our relative error is estimated to be of the order of ±2%, the experimental value is clearly not accounted for by quadrupole-induced dipole forces.

Foreign-gas broadening by rare gases is expected to be dominated by quadrupole-induced dipole forces.[27,28] It is surprising that this force should dominate over the longer-range interaction of dipole-induced dipole. It can be shown, however, that the symmetry of the dipole-induced dipole term is such that it provides no inversion transitions and hence a small contribution to the linewidth. Anderson has used this term to obtain fairly good agreement for the NH_3 linewidth broadened by argon and helium.

Finally, note from Table IV that all of the foreign-gas optical-broadening cross sections are less than the gas kinetic cross sections. This has two implications: The approximation of straight-line trajectories used by Anderson is no longer valid, and the collisional processes involved do not significantly perturb the internal coordinates leading to the possibility of observing collisional narrowing of the residual Doppler width.

B. Pressure shift in NH_3

As described in Sec. III H of Ref. 1, a pressure shift in the center frequency of a line can give us additional information about *elastic* collisional processes not available from line-broadening studies. For the case of NH_3 microwave transitions, we would expect no pressure shift in first order for self-broadening. The reasons are twofold. The matrix elements are not diagonal in the inversion quantum number, and hence dipole-dipole forces cause state changes; and both our upper and lower rotational states are the same, since we are dealing with a $Q(\Delta J=0)$ transition. The second reason is valid in the microwave region, but is considered inapplicable for our case, since the inversion splitting is much larger in the upper state ($\nu_2=2$) than in the lower state, leading to a difference in the collisional shift of each level. For broadening by foreign-gas perturbers examined in this study, the only case exhibiting a resolvable pressure shift was that of NH_3-Ne collisions. These data are presented in Fig. 6, giving a value for the shift of 0.38 MHz/Torr. This shift is a large fraction ($\frac{2}{3}$) of the broadening coefficient (line S_1 in Fig. 5). As explained in Ref. 1, the pressure shift samples only collisional processes which are elastic. Since the quadrupole-induced dipole force accounts for the broadening of NH_3-rare gas by causing transitions between the inversion doublet, we are led to postulate that the dominant force involving elastic collisions is the dipole-induced dipole force. Since this is a longer-range force than the quadrupole-induced dipole force, it could account for the observed pressure shift.

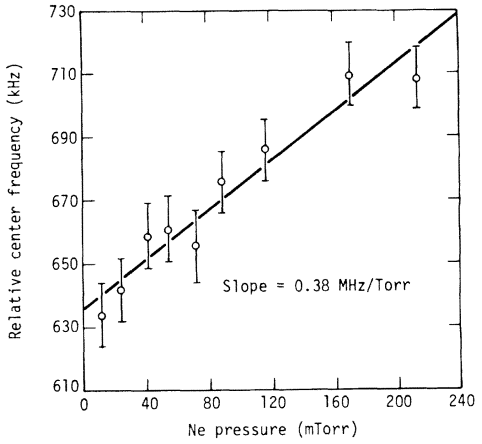

FIG. 6. NH_3-He pressure shift in the center frequency of the two-photon transition $(J,K,M) \rightarrow (J',K',M') = (5,4,5) \rightarrow (5,4,5)$. The indicated error bars are 20 kHz. The slope of this line is 0.38 MHz/Torr.

C. Collisional narrowing in NH_3

One final observation concerning collisional effects in NH_3 is the observation of collisional narrowing of the residual Doppler width. The most pronounced observation is given in Fig. 5 for NH_3-Ne collisions. Note that a straight-line fit through low-pressure points (S_2 in Fig. 5) actually gives a negative slope for the pressure-broadening coefficient. The actual narrowing that occurs is 70 kHz. This is the first observation of collisional

narrowing in two-photon absorption spectroscopy. A narrowing of this magnitude is significant when one considers that the total linewidth is a convolution of a Doppler width (~1.35 MHz) and a homogeneous width (~1.6 MHz). An anomalously low broadening coefficient was also observed for the low-pressure points of NH_3-He collisions; however, a narrowing was not observed in this case.

Collisional narrowing was first predicted by Dicke[18] and has since been included in a large number of theories of combined Doppler and pressure broadening. Dicke's basic assumption is that the total effect of a collision is to change the radiator's velocity without a perturbation of the internal coordinates. Under these conditions a Doppler-broadened line can show considerable narrowing as the pressure is increased. This effect has been experimentally demonstrated in water vapor[30] and in the vibrational Raman lines[31] of H_2.

For the case of NH_3-Ne collisions, we see that the straight-line fit to the high-pressure points (S_1 in Fig. 5) gives a very low broadening coefficient. This indicates that collisions do not strongly perturb the internal motions, and hence that this would be a good system for the observation of collisional narrowing. Also note that the normal pressure range where these effects can be seen is in the region 10–100 Torr.[30] However, since Δk is considerably reduced by the two-photon effect (~15 cm^{-1}), this effect can be observed at much lower pressures. Hence it is reasonable that we see some narrowing effect. Since our linewidth is not a purely Doppler-broadened line, we can extract no information as to the value of the particle diffusion coefficient for NH_3-Ne collisions (see, for example, Ref. 30).

IV. MEASUREMENTS OF VIBRATIONAL TRANSITION DIPOLE MATRIX ELEMENTS IN NH_3

A. Introduction

In addition to the collisional effects observed and discussed in Sec. III, the DFTPA experiment also provided the necessary experimental data to determine two different vibrational transition dipole matrix elements in the ν_2 mode of NH_3 not previously measured. Two different effects were used to make these measurements. The $1^+ \rightleftarrows 2^-$ transition moment was estimated using the optical Stark effect, while the $2^+ \rightleftarrows 2^-$ transition moment was measured using the second-order Stark effect arising from the applied dc electric field. The results of this section are summarized in Table V along with a comparison with the known transition moments.

TABLE V. Vibrational transition dipole matrix elements measured for the ν_2 mode in NH_3.

Transition	$\delta\mu$ (D)	Reference
$0^- \rightleftarrows 1^+$	0.23 ± 0.02	6
$1^+ \rightleftarrows 2^-$	0.27 ± 0.05	This work
$0^+ \rightleftarrows 0^-$	1.475 ± 0.006	5
$1^+ \rightleftarrows 1^-$	1.25 ± 0.01	5
$2^+ \rightleftarrows 2^-$	0.83 ± 0.08	This work

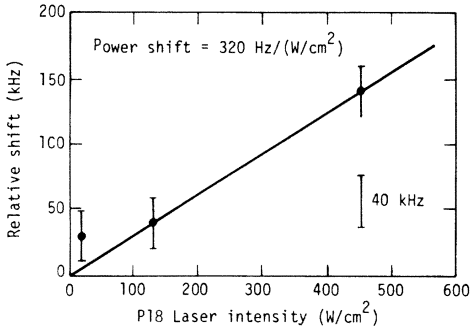

FIG. 7. Shift of the two-photon transition frequency in NH_3 as a function of the $P18$ laser power. The shift determined by these data is that of the upper state $(\nu_2, J, K, M) = (2^-, 5, 4, 5)$. This enables the calculation of the $1^+ \rightarrow 2^-$ transition dipole moment. For these calculations, the laser was focused to a beam waist of 0.81 mm, giving a peak intensity of 390 W/cm^2.

B. $1^+ \rightleftarrows 2^-$ transition

The optical Stark effect was used to determine the transition dipole matrix element of the $1^+ \rightarrow 2^-$ transition. This effect is commonly known as an "optical power shift" and can be experimentally observed as a shift in the center frequency of a two-photon transition as a function of the intensity of the pump laser. Data demonstrating this effect in NH_3 is given in Fig. 7 for the two-photon transition $(\nu_2, J, K, M) \rightarrow (\nu_2', J', K', M') = (0^-, 5, 4, 5) \rightarrow (2^-, 5, 4, 5)$. Here, the center frequency of the two-photon transition is plotted versus the intensity of the $P18$ laser line (see Fig. 2). These data were taken to provide a correction factor for the exact value of the two-photon transition frequency. The experimental procedure entailed placing an aperture in the probe beam such that the only intensity reaching the detector was the uniform center portion of the mode. This prevented the Gaussian intensity distribution from affecting the overall observed shift. Using the measured beam diameters, we determine a power shift for the $(\nu_2, J, K, M) = (2^-, 5, 4, 5)$ level of 320 Hz/(W cm^{-2}). The errors in this measurement result mainly from the inaccuracy in the actual beam intensities in the cell. These errors are estimated to be ±20%. This is the first observation of these types of shifts in the infrared, although a similar experiment was

performed in the visible and reported by Liao and Bjorkholm.[32]

A theoretical expression for this shift can be written, using second-order perturbation theory and assuming one dominant intermediate state, as[33]

$$\Delta W_n = \frac{1}{4}\left(\frac{|\langle n|\vec{\mu}|m\rangle\cdot\vec{E}_0|^2}{W_n^0 - W_m^0 - h\nu} + \frac{|\langle n|\vec{\mu}|m\rangle\cdot\vec{E}_0|^2}{W_n^0 - W_m^0 + h\nu}\right), \tag{12}$$

where the state n corresponds to $(\nu_2, J, K, M) = (2^-, 5, 4, 5)$, the state m to $(1^+, 5, 4, 5)$ and the laser radiation field E_0 to the $P18$ CO_2 laser line. Since $|W^0_{(2^-)} - W^0_{(1^+)}| < h\nu(P18)$, we need take only the first term of Eq. (12). Therefore Eq. (12) reduces to

$$\Delta W_{(2^-)} = \tfrac{1}{4}\,|\langle 2^-|\vec{\mu}|1^+\rangle\cdot\vec{E}_0|^2/(W^0_{(2^-)} - W^0_{(1^+)} - h\nu). \tag{13}$$

We do not consider the power shift of the lower state ($\nu_2 = 0^-$), because the power of only the $P18$ line was varied. From Fig. 7 the power shift of the 2^- level ($\Delta W_{(2^-)}$) was measured to be 124 kHz at 4 W of $P18$ laser power. The intensity of the laser field for a fundamental transverse mode is given by

$$I = 2P/\pi\omega^2, \tag{14}$$

where P is the laser power and ω is the average beam radius within the Stark cell, which was calculated to be 0.81 mm for the $P18$ line. At a power of 4 W this corresponds to an intensity of 390 W/cm^2 with an electric field amplitude E_0 of 540 V/cm. The resonance denominator $(W^0_{(2^-)} - W^0_{(1^+)} - h\nu)$ is calculated to be ~4950 MHz when the dc Stark field is present.

The transition dipole matrix element $\langle 2^-|\mu|1^+\rangle$ of Eq. (13) is composed of two parts, the vibrational transition dipole matrix element $\delta\mu$ to be determined, and the direction-cosine matrix element $\Phi_{J,K,M}$, which arises from the known angular parts of the wave functions.[11] We can then write

$$\langle 2^-|\mu|1^+\rangle = \delta\mu\Phi_{J,K,M}. \tag{15}$$

For the transition $(J, K, M) \rightarrow (J', K', M') = (5, 4, 5) \rightarrow (5, 4, 5)$, $\Phi_{J,K,M} = 0.666$. Therefore we may solve Eq. (13) for $\delta\mu$, yielding

$$\delta\mu(1^+ \rightleftharpoons 2^-) = [4\Delta W_{(2^-)}(W^0_{(2^-)} - W^0_{(1^+)} - h\nu)/a^2(\Phi_{J,K,M})^2 E_0^2]^{1/2}, \tag{16}$$

where $a = 0.503\,48$ is the conversion constant previously mentioned in Eq. (3). Substitution of the above described values in Eq. (16) gives

$$\delta\mu(1^+ \rightarrow 2^-) = 0.27 \pm 0.05 \text{ D}. \tag{17}$$

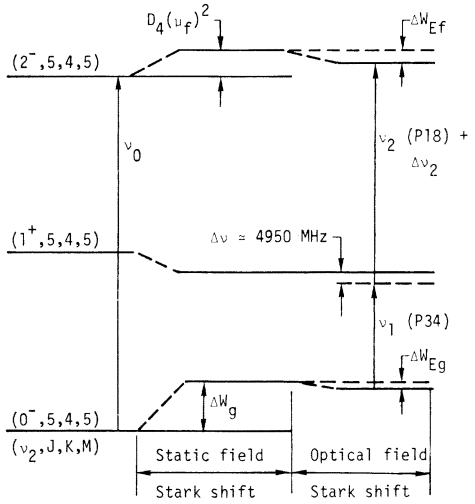

FIG. 8. Schematic of two-photon absorption transition in NH_3, indicating the static Stark- and power-shift corrections used to calculate the vibrational transition dipole matrix element of the $\nu_2 = 2^+ \rightleftharpoons 2^-$ transition.

As seen in Table V, this transition dipole moment is larger than that of the lower state $[\delta\mu(0^- \rightarrow 1^+) = 0.23$ D], but less than the value calculated by a harmonic-oscillator model which is proportional to the square root of the vibrational quantum number v,[34] i.e.,

$$\delta\mu(-2) = \delta\mu(0 \rightarrow 1)\,v^{1/2} \simeq (0.23)\,2^{1/2} \simeq 0.33 \text{ D}.$$

Nevertheless, a value of 0.27 D for the $1^+ \rightleftharpoons 2^-$ transition seems quite reasonable in view of the fact that the ν_2 mode is strongly anharmonic.

C. $2^+ \rightleftharpoons 2^-$ transition

The vibrational transition dipole moment of the $2^+ \rightleftharpoons 2^-$ transition was measured using a method similar to that used to calculate the resonant frequency of the $(\nu_2, J, K) = (0^-, 5, 4) \rightarrow (2^-, 5, 4)$ transition, as discussed in Sec. II C. Refering to Fig. 8, the center frequency of the two-photon transition is given by

$$\nu_0 = \nu_1 + \nu_2 + \Delta\nu_2 + \Delta W_g + \Delta W_{Eg} - D_5(\mu_f)^2 - \Delta W_{Ef}, \tag{18}$$

where ΔW_g is the sum of the first- ($\Delta W_g^{(1)}$) and second-order ($\Delta W_g^{(2)}$) dc Stark shifts of the lower level, $D_5(\mu_f)^2$ is the dc Stark shift of the upper level containing the unknown dipole moment, ΔW_E is

the power shift correction (here we have assumed ΔW_E positive in the vertical direction), and $\Delta\nu_2$ is the resonance frequency offset of one of the lasers ($P18$ line) from its line center (see Table III). Since all of the $M_g \rightarrow M_f$ transitions yield the same two-photon absorption frequency ν_0, Eq. (18) can be equated for different $M_g \rightarrow M_f$ transitions. Solving for μ, we have

$$\mu_f = \left(\frac{(\Delta W_g - \Delta W_g') + (\Delta\nu_2 - \Delta\nu_2') + (\Delta W_{Eg} - \Delta W_{Eg}') + (\Delta W_{Ef}' - \Delta W_{Ef})}{D_5 - D_5'} \right)^{1/2}, \tag{19}$$

where the unprimed and primed variables denote different $M_g \rightarrow M_f$ transitions. All of the expressions in Eq. (19) have been previously calculated (see Table II) except the power shift terms (ΔW_{Eg} and ΔW_{Ef}).

To calculate the power shifts of the 0^- and 2^- levels we will use Eq. (12) with only one dominant intermediate state corresponding to the vibrational level $\nu_2 = 1^+$. The 0^- level is affected primarily by its interaction with the $P34$ line, which has a power of 2 W with an average beam radius of 0.76 mm in the Stark cell. Employing Eq. (14), we find the $P34$ laser line intensity to be 220 W/cm^2, corresponding to an electric field amplitude of 410 V/cm. The vibrational transition dipole matrix element between the 0^- and 1^+ intermediate is $\delta\mu = 0.23$ D. The resonance denominator remains 4950 MHz. The direction-cosine matrix elements may be found in Ref. 11. The resulting values for the 0^- power shift are listed in Table VI. In order to calculate the power shift of the 2^- level associated with the interaction of the $P18$ line, we will use the experimental parameters previously mentioned in Sec. IV B, including our calculated value of $\sigma_1 = 0.27$ D for the $1^+ \rightarrow 2^-$ vibrational transition dipole moment.

TABLE VI. Optical power shifts for the 0^- and 2^- levels of the ν_2 mode in NH_3.

0^- level			2^- level		
M_g	M_i	W_{Eg} (kHz)	M_i	M_u	W_{Ef} (kHz)
5	5	−50	5	5	−121
4	4	−32	4	4	−77
3	3	−18	3	3	−44

The results of these calculations also may be found in Table VI. Having determined the appropriate optical power shifts of the $\nu_2 = 0^-$ and $\nu_2 = 2^-$ levels, we are now in a position to evaluate Eq. (19). This calculation is tabulated in Table VII for various permutations of the $M_g \rightarrow M_f = 5 \rightarrow 5$, $4 \rightarrow 4$, and $3 \rightarrow 3$ transitions. The average value of μ as taken from Table VII is 0.83 ± 0.08 D, where we have statistically weighted the permutations $(M, M') = (5,3) : (5,4) : (4,3)$ as $3 : 1 : 2$, commensurate with the experimental accuracy. This measured dipole moment of the $\nu_2 = 2$ level represents the vibrational transition dipole matrix element between the $\nu_2 = 2^- \rightleftarrows 2^+$ levels. This matrix element therefore is assigned the value

$$\delta\mu(2^- \rightleftarrows 2^+) = 0.83 \pm 0.08 \text{ D}.$$

Since this transition dipole matrix element has not been previously measured, a comparison with other measurements is not possible. However, Gille and Lee[3] used an estimate of $\delta\mu(2^- \rightleftarrows 2^+) \simeq 1.0$ D in calculating line intensities for this transition. Shown in Table V are the vibrational transition dipole matrix elements measured for the ν_2 mode in NH_3, with a comparison to other work. It is in-

TABLE VII. Evaluation of $(2^- \rightleftarrows 2^+)$ vibrational transition dipole matrix element of the ν_2 mode in NH_3.

Transition				$\Delta W_g - \Delta W_g'$ [a]	$\Delta\nu_2 - \Delta\nu_2'$ [b]	$\Delta W_{Eg}' - \Delta W_{Eg}$ [c]	$\Delta W_{Ef} - \Delta W_{Ef}'$ [c]	$D_5 - D_5'$ [d]	μ
M_g	M_f	M_g'	M_f'	(kHz)	(kHz)	(kHz)	(kHz)	(kHz D^2)	(D)
5	5	3	3	−862	496	−32	77	−466	0.830
5	5	4	4	−1134	972	−18	44	−149	0.955
4	4	3	3	272	−476	−14	33	−317	0.764
								Average [e]	$= 0.83 \pm 0.08$

[a] See Table II.
[b] See Table III.
[c] See Table VI.
[d] $D_5 = D_4 E^2$, where D_4 and E are given in Table II.
[e] This average is weighted according to experimental error by the following formula: $(M, M') = (5,3) : (5,4) : (4,3) = 3 : 1 : 2$.

teresting to note the dependence of these transition moments with the ν_2 quantum number. As the quantum number becomes larger, the dipole moment is reduced, approaching values similar to typical infrared-moment transitions.

D. Discussion of the optical power shift

Although the optical power shift was used to determine the vibrational transition dipole matrix element for the $1^+ \rightleftarrows 2^-$ transition, it contains some interesting features that require further discussion. It may be noted that the optical power shift terms (ΔW_E) listed in Table VI are negative for both the $\nu_2 = 0^-$ and 2^- levels. The negative value of the sift is associated with the fact that the intermediate state, $\nu_2 = 1^+$, lies at a higher energy than that corresponding to the ν_1 quantum ($P34$ line in Fig. 8). If the energies of the intermediate state and the first laser photon were reversed, the optical power shifts would then be positive. Also apparent from Table VI is the fact that of the optical power shift of the upper level $\nu_2 = 2^-$ is greater than that of the lower level, $\nu_2 = 0^-$. The reason for this is twofold. We are operating the $P18$ laser line at a higher intensity (4 W) than the $P34$ laser line (2 W), and thus the amplitude E_0 in Eq. (13) is larger, and the vibrational transition dipole matrix element $\delta\mu = 0.27$ D for the transition $1^+ \rightarrow 2^-$ is larger than the corresponding matrix element, $\delta\mu = 0.23$ D, for the $0^- \rightarrow 1^+$ transition.

These particular features point to an interesting technique for tuning a molecular transition into or out of resonance using these multiphoton processes. From Fig. 8 and Eq. (13), one can easily visualize that if the laser intensities of one or both of the ν_1 and ν_2 radiation fields are of sufficient intensity, it could be feasible to tune the two-photon transition into resonance using only the optical power shift. This technique would be particularly advantageous in NH_3 and other molecular gases which have a low dc electric field breakdown threshold. Elimination of the dc Stark tuning would facilitate working at higher gas pressures, a situation very favorable for two-photon excitation schemes. A calculation of the power necessary to tune the two-photon transition into resonance indicates that *only* $\sim 10^6$ W/cm^2 would be necessary. These powers are relatively easy to attain by combining stable laser systems with multipass TEA CO_2 laser amplifiers.[35] There has also been a recent proposal to combine this optical Stark effect with an adiabatic rapid passage to completely invert a two-photon transition.[36] Use of these types of techniques could have direct application to laser photochemistry and laser-induced isotope separation.

V. SUMMARY AND CONCLUSIONS

To summarize, we have reported the observation of Doppler-free two-photon absorption in the molecular system of NH_3. Using the two-photon techniques described in Ref. 1, we have determined both spectroscopic and collisional properties of this molecular system. This information falls into five basic categories.

1. *Accurate measurement of two-photon transition frequencies.* The NH_3 transition of $(\nu_2, J, K) = (0^-, 5, 4) \rightarrow (2^-, 5, 4)$ has been measured to be $1876.991\,493 \pm 3 \times 10^{-6}$ cm^{-1}. This transition is now known to about three parts in 10^9 (the accuracy of the speed of light) and could now be used as a secondary frequency standard.

2. *Determination of pressure-broadening coefficients.* We can do this for the two-photon transition described above for the cases of NH_3 broadened by NH_3, H_2, D_2, He, Ne, and Xe. These values can be found in Table IV.

3. *Observation of a pressure shift.* A pressure shift is observed in the center frequency of the two-photon transition for NH_3 broadened by Ne.

4. *Measurement of two vibrational transition dipole moments in NH_3.* $1^+ \rightarrow 2^-$ was measured to be 0.27 D and was obtained from the power-shift data in Fig. 7. $2^+ \rightarrow 2^-$ was measured to be 0.83 D and was obtained from second-order Stark tuning of the various $\Delta M = 0$ two-photon transitions.

5. *Observation of the collisional narrowing.* This is observed in the residual Doppler profile for NH_3-Ne collisions.

It is important to observe that all of these measurements required the complete specification of all of the degrees of freedom of the radiation field. These included stable CO_2 frequencies for spectroscopic measurements, utilization of the wave vector (direction of propagation) for the Doppler-free effect, utilization of the polarization to observe the different ΔM two-photon transitions, and utilization of the intensity and mode quality for the power shift measurements. The CO_2 oscillator is one of the few laser systems which has all of these properties sufficiently well characterized to be able to make measurements of this type.

As a final note, we feel that the techniques of Doppler-free two-photon absorption with fixed frequency sources can be applied generally to a large number of molecular systems. Not only has it been demonstrated that a new and powerful tool has been added to the repertoire of experimental spectroscopic techniques, but that major contributions to experimental collision physics can also be achieved. Furthermore, it is apparent that Doppler-free many-photon excitation schemes will have a major impact on laser isotope separation in situations where the isotopic transitions of interest are

masked by the Doppler width and several quanta are required for excitation. Applications of this nature will presumably be demonstrated within the near future.

ACKNOWLEDGMENT

The authors gratefully acknowledge the tireless and expert technical contributions of B. R. Schleicher.

---

†Work performed under the auspices of the U. S. Energy Research and Development Administration.

*Present address: Molecular Physics Center, Stanford Research Institute, Menlo Park, Calif. 94025.

‡Present address: HQ. 15th Engineer Bn., Fort Lewis, Wash. 98433.

[1]William K. Bischel, Patrick J. Kelly, and Charles K. Rhodes, preceding paper, Phys. Rev. A 13, 1817 (1976).

[2]F. W. Taylor, J. Quantum. Spectrosc. Radiat. Transfer 13, 1181 (1973).

[3]John C. Gille and Tay-How Lee, J. Atmos. Sci. 26, 932 (1969).

[4]J. S. Garing, H. H. Nielsen, and K. Narahari Rao, J. Mol. Spectrosc. 3, 496 (1959).

[5]F. J. Shimizu, J. Chem. Phys. 51, 2754 (1969); 52, 3572 (1970).

[6]H. M. Mould, W. C. Price, and G. R. Wilkinson, Spectrochim. Acta 15, 313 (1959).

[7]T. Shimizu, F. O. Shimizu, R. Turner, and T. Oka, J. Chem. Phys. 55, 2822 (1971).

[8]W. S. Benedict, Earle K. Plyler, and E. D. Tidwell, J. Chem. Phys. 29, 829 (1958).

[9]Gerhard Herzberg, *Infrared and Raman Spectra of Polyatomic Molecules* (Van Nostrand-Reinhold, New York, 1945).

[10]W. S. Benedict, Earle K. Plyler, and Eugene D. Tidwell, J. Res. Natl. Bur. Stand. 61, 123 (1959).

[11]C. H. Townes and A. L. Schawlow, *Microwave Spectroscopy* (McGraw-Hill, New York, 1955).

[12]W. S. Benedict and E. K. Plyler, Can. J. Phys. 35, 1235 (1957).

[13]J. W. C. Johns, A. R. W. McKellar, and A. Trombetti, J. Mol. Spectrosc. 55, 131 (1975); R. E. Walker and B. F. Hochheimer, *ibid.* 34, 500 (1970).

[14]W. H. Weber, P. D. Makes, K. F. Yeung, and C. W. Peters, Appl. Opt. 13, 1431 (1974).

[15]B. D. Fried and S. D. Conte, *The Plasma Dispersion Function* (Academic, New York, 1961).

[16]W. Gordy and R. L. Cook, *Microwave Molecular Spectra* (Wiley, New York, 1970).

[17]P. L. Kelley, H. Kildal, and H. R. Schlossberg, Chem. Phys. Lett. 27, 62 (1974).

[18]R. H. Dicke, Phys. Rev. 89, 472 (1953).

[19]P. W. Anderson, Phys. Rev. 76, 647 (1949).

[20]B. Bleaney and R. P. Penrose, Proc. R. Soc. A 189, 358 (1947).

[21]Robert L. Legan, James A. Roberts, Edgar A. Rinehart, and Chun C. Lin, J. Chem. Phys. 43, 4337 (1965).

[22]R. K. Kakar and R. L. Poynter, J. Mol. Spectrosc. 54, 475 (1975).

[23]P. Varanasi, J. Quant. Spectrosc. Radiat. Transfer 12, 1283 (1972).

[24]A. T. Mattick, A. Sanchez, N. A. Kurnit, and A. Javan, Appl. Phys. Lett. 23, 12 (1973).

[25]Takeshi Oka, J. Chem. Phys. 48, 4919 (1968).

[26]J. W. C. Johns, A. R. W. McKellar, T. Oka, and M. Romheld, J. Chem. Phys. 62, 1488 (1975).

[27]Direct measurement for the $s \rightarrow a$ $Q(J=5, K=5)$ transition has shown that the collisional lifetime of the excited $\nu_2 = 1$ vibration is five times longer than that of the ground state. For details, see Michael M. T. Loy, Phys. Rev. Lett. 32, 814 (1974).

[28]William V. Smith, J.Chem. Phys. 25, 510 (1956).

[29]Vinod Prakosh Krishnagi, Rev. Mod. Phys. 38, 690 (1966); Daniel E. Strogryn and Alex P. Strogryn, J. Mol. Phys. 11, 371 (1966).

[30]R. S. Eng, A. R. Calawa, T. C. Harman, P. L. Kelly, and A. Javan, Appl. Phys. Lett. 21, 303 (1972).

[31]J. R. Murray and A. Javan, J. Mol. Spectrosc. 42, 1 (1972).

[32]P. F. Liao and J. E. Bjorkholm, Phys. Rev. Lett. 34, 1 (1975).

[33]S. H. Autler and C. H. Townes, Phys. Rev. 100, 703 (1955); A. M. Bonch-Breuvich and V. A. Khodovoi, Usp. Fiz. Nauk 93, 71 (1967) [Sov. Phys.-Usp. 10, 637 (1968)].

[34]E. B. Wilson, Jr., J. C. Decius, and P. C. Cross, *Molecular Vibrations, The Theory of Infrared and Raman Vibrational Spectra* (McGraw-Hill, New York, 1955).

[35]H. Kogelnik and T. J. Bridges, IEEE J. Quantum Electron. QE-3, 95 (1967).

[36]D. Grischkowsky and M. M. T. Loy, Phys. Rev. A 12, 1117 (1975).